

Preparation of Ag-deposited porous TiO₂ films using polystyrene nanoparticles as templates for enhanced photocatalysts

Yeeun Kang, Kyungho Song, Jun-Hwan Park, Young Chai Kim and Seong-Geun Oh*

Department of Chemical Engineering, Hanyang University 222 Wangsimni-ro, Seongdong-gu, Seoul 133-791, Republic of Korea

Titanium dioxide (TiO₂) is used as a photocatalyst in such processes as industrial wastewater treatment since it is a large-band-gap semiconductor with a catalytically active surface. For improvement of photocatalytic activity, many developments of TiO₂ have been studied with physical and chemical modifications. In this study, the monodisperse polystyrene colloid was prepared via emulsion polymerization, then the porous TiO₂ inverse opal (TIO) film was manufactured through dip coating process using polystyrene (PS) as templates. The inverse opal structure has a large surface area and it makes to improve the photocatalytic performance of TiO₂. After that, a small amount of silver nanoparticles were deposited on the surface of TIO films through photodeposition method to inhibit charge carrier recombination and increase the photocatalytic activity. This silver-deposited TIO film can be used as an enhanced photocatalyst. The resultant samples were characterized by TEM, DLS, FE-SEM, XPS, EDS, and UV-Vis spectroscopy. Furthermore, photocatalytic performance was analyzed by photodegradation of methylene blue dye in aqueous solutions.

Key words: Porous TiO₂ film, Polystyrene colloid, Inverse opal structure, Ag deposition, Photocatalyst.

Introduction

TiO₂ is a very promising material because it has special properties such as wide band gap, low cost, nontoxicity, and high chemical stability. Therefore, they have been used in wide application fields including dye sensitized solar cells [1], gas sensor [2], lithium batteries [3], and photocatalyst [4]. Among the various applications of TiO₂, photocatalysis is one of the most interesting fields and its development is going along recently because of the concern over the water contaminations by volatile organic compounds (VOCs) which can threaten the environment and human health seriously. The mechanisms of photocatalytic reaction have been studied widely. In short, when TiO₂ absorbs light with energy higher than the band gap, electron-hole pairs are generated and then electrons are excited from the valence band to the conduction band. These separated charge carriers migrate toward the surface where they can be trapped or react with the solution species. As reactive oxygen species are formed by oxidation onto the surface of TiO₂, the organic pollutants adsorbed on the surface are decomposed and mineralized into CO₂, H₂O and inorganic ions [5, 6]. From the environmental point of view, this photodecomposition process is very useful and effective because the harmful pollutant can be decomposed to non-harmful compounds. However, TiO₂ shows a

low spectral response to visible light because of its wide band gap [7] and the recombination of the generated electron and hole occurs which can lower the photocatalytic activity [8]. Therefore, for improving light absorption properties and decreasing the electron-hole combination rate, many efforts have been studied. One of them is a formation of porous or other 3D-complex structures instead of conventional compact structure [9-11]. The inverse opal structure can improve the light absorption property especially due to its large surface area and multiple scattering effect of the large pore size. Another approach is the chemical modification by deposition of the noble metals such as Au, Pt, Pd, and Ag on the surface of TiO₂ [12-14]. Since the deposited noble metals act as traps to capture the photoinduced electrons, the electron-hole recombination can be reduced [15, 16]. Moreover, the capability of light absorption can be increased due to the surface plasmon absorption (SPA) effect of immobilized metal nanoparticles [17].

In this study, we prepared the TiO₂ inverse opal (TIO) films through dip coating process using polystyrene (PS) templates. As mentioned above, the inverse opal structure has large surface area and it makes to improve the photocatalytic performance of TiO₂. Then, a small amount of Ag nanoparticles was introduced on the surface of TIO films through photo deposition method. Both physical and chemical modifications have a strong influence on the efficiency of the photocatalytic activity of TiO₂, therefore, this Ag-deposited TIO film can be used as an enhanced photocatalyst.

*Corresponding author:
Tel : +82-2-2220-0485
Fax: +82-2-2294-4568
E-mail: seongoh@hanyang.ac.kr

Materials and Methods

Materials

For synthesis of porous TiO₂ films, we used titanium (IV) butoxide (Ti(OBu)ⁿ₄, Aldrich), 1-butanol (Junsei), acetylacetone (AcAc, Aldrich), and diluted nitric acid (60%, HNO₃, Samchun). For preparation of polystyrene colloid, styrene monomer (Sigma-Aldrich), 4-styrene sulfonate sodium salt (Sigma-Aldrich), sodium bicarbonate (Sigma-Aldrich), and potassium persulfate (KPS, Sigma-Aldrich) were used as a monomer, a co-monomer, a buffer, and an initiator, respectively. The (3-aminopropyl) trimethoxysilane (APTMS, Fluka), silver nitrate (AgNO₃, Showa), and 2-propanol (Samchun) were used for the modification of TIO films by metal nanoparticles. Slide glasses were cleaned with sonication process using 2-propanol and acetone before fabrication of films. In addition, for the evaluation of photocatalytic activities of prepared films, methylene blue (MB, Daejung) was used as a target material. Ultrapure Milli-Q water was used in all experiments.

Preparation method

Synthesis of monodisperse TiO₂ colloid

The TiO₂ colloid was synthesized by modified sol-gel method. Ti(OBu)ⁿ₄ as a precursor was mixed with AcAc as a chelating agent with 1:4 molar ratio in order to control the hydrolysis/condensation reaction by chelating reaction [18]. After stirring for a while at room temperature, the mixture was added to 30 mL of 1-butanol. The solution was stirred for 15 min, after which a diluted aqueous solution of nitric acid was added dropwise ([H⁺]/[Ti] = 0.2, [H₂O]/[Ti] = 10, molar ratio). The colloidal dispersion was aged overnight at 60 °C to get the transparent sols.

Preparation of TIO film using PS templates

PS spherical particles were chosen as templates because they are self-assembled for a well-ordered multi-layer to fabricate the template for TIO films. The PS colloid was synthesized by emulsifier-free emulsion polymerization method as described in the literature [19]. Briefly, 49 g of styrene, 0.18 g of 4-styrene sulfonate sodium salt, 0.15 g of sodium hydrogen carbonate, and 0.15 g of KPS were mixed in 270 g of deionized water. This mixture was stirred for 1 hr at room temperature and then placed into an oil bath maintained at 80 °C. The polymerization proceeded for 24 h under nitrogen atmosphere. The stirring rate was 200 rpm using mechanical stirrer. Using prepared 130 nm-PS colloid, PS template film was prepared by a dip coating process. A cleaned slide glass was immersed vertically in the center of PS colloid and pulled out from the sol and then dried for 30 min at 70 °C in an oven. The cycles of coating and drying were repeated 4 times to prepare the thicker template. Next, PS-array film was dipped into TiO₂ transparent colloidal solutions for

Table 1. Designation of various samples.

	TIO	AT10	ATA10	AT30	ATA30
APTMS treatment	Non-treated	Non-treated	Treated	Non-treated	Treated
UV irradiation time during photodeposition	No irradiation	10 min		30 min	

10 min and pulled out. Then, the film was placed at room temperature for 1 day to dry completely. This TiO₂ infiltration step was repeated 2 times for sufficiently filling to the voids in the template. The resulting films were sintered at 450 °C for 2 hrs (1 °C/min) to remove the PS template and then the TIO films were fabricated.

Surface modification by APTMS treatment of TIO film

The organosilane APTMS is well known to be quickly chemisorbed onto the surfaces of titania containing -OH groups via strong covalent bonds of Si-O-Ti [20]. It forms homogeneous self-assembled monolayers with terminated amino-functional group which is used as a linkage unit to attach other functional molecules including various metal particles [21]. Therefore, the influence of the APTMS treatment on Ag coating process was also investigated. The TIO films were immersed into the 1 wt.% aqueous APTMS solution and heated at 60 °C for 1 hr. The TIO films modified by APTMS were rinsed with distilled water and dried at 55 °C in the oven.

Deposition of Ag nanoparticles on the TIO film

Ag nanoparticles were immobilized on TIO samples via a photodeposition method. The pure TIO and APTMS-treated TIO films were immersed in a 1 mM Ag precursor aqueous solution containing 10 vol.% of 2-propanol, which could help the reduction of Ag. The obtained Ag-deposited TIO films were washed with distilled water and then dried in the oven. These samples are designated according to APTMS treatment and UV irradiation time as shown in Table 1. For comparison of the optical properties, TiO₂ compact thin film with the thickness of 500 nm, which was used as reference materials, was prepared by spin coating using the synthesized TiO₂ colloid.

Characterization

The field emission scanning electron microscopy (FE-SEM, JSM-6700F, JEOL Co.) and transmission electron microscopy (TEM, JEM-2100F, JEOL Co.) were used to investigate the morphology of resultant samples. The dynamic light scattering (DLS; Malvern instruments, Zetasizer Nano ZS) was used to detect the particles in solution and confirm the solution stability. The selected area electron diffraction (SAED; attached to TEM equipment) patterns were obtained for

measurement of lattice spacing values of crystalline particles. The chemical state of Ag-deposited TiO films was investigated by X-ray photoelectron spectroscopy (XPS, Thermo Fisher Scientific co., theta probe base system) and energy-dispersive X-ray spectroscopy (EDS; attached to FE-SEM equipment). The absorption property of each sample was measured by UV-Vis spectrophotometer (Agilent Technologies, Agilent 8435).

Evaluation of the photocatalytic activity

To evaluate the photocatalytic activity of the prepared samples, the photodegradation of MB in aqueous solution was carried out under UV-light irradiation. The samples were settled in a 5 ppm MB solution in each plastic cell. The reaction temperature was kept at room temperature to prevent any thermal catalytic effect. The MB solutions with samples were left for 30 min in the dark to achieve adsorption/desorption equilibrium between photocatalyst and MB before irradiation and subsequently the reaction was started with UV irradiation. The concentration of MB in each sample was monitored using its maximum absorbance at 665 nm from the UV-Vis absorption spectrum measured after a certain period of irradiation. Then, the relative concentration C/C_0 of MB in solution was plotted against UV-light irradiation time.

Results and Discussion

Analysis of TiO₂ colloid

TiO₂ colloid synthesized by modified sol-gel method with AcAc was investigated by TEM and the result is shown in Fig. 1(a). Dark spherical particles which were

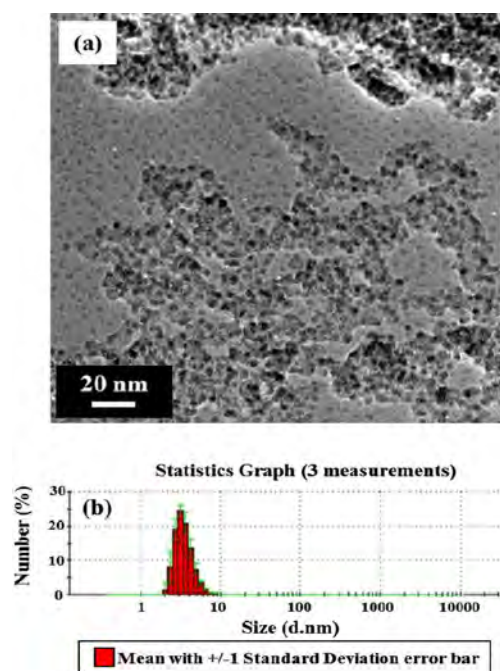


Fig. 1. (a) TEM image and (b) DLS data of TiO₂ particles synthesized by modified sol-gel method with AcAc.

TiO₂ nanoparticles were observed with the average size of 5 nm and narrow size distribution. Translucent compounds surrounding TiO₂ nanoparticles were also found and it is expected that AcAc protect the aggregation of TiO₂ nanoparticles by coating them. DLS analysis was conducted to verify the size of synthesized TiO₂ particles (Fig. 1(b)). The average size of TiO₂ particles was about 5 nm with narrow size distribution, which was in a good agreement with the TEM image.

Analysis of morphological property of PS template and TiO film

The PS opal template was prepared on the slide glass from self-assembled spherical and monodisperse PS nanoparticles. In Fig. 2(a-c), the size of PS particles was 130 nm and the thickness of PS template was approximately 2.5 μm. The 3D-ordered TiO structure was obtained after dipping the template in the TiO₂ colloid and calcination at 450 °C for 2 hrs. The FE-SEM and TEM images of the fabricated films were illustrated in Fig. 2(d-f). The pore diameter of TiO film was about 114 nm as shown in Fig. 2(f). The size of pores was smaller than that of the original PS particles. This is because the shrinkage of structure occurred during the calcination.

Ag nanoparticles were coated on the surface of TiO film via photodeposition process under UV irradiation. When UV was irradiated to the TiO film which was immersed in the Ag precursor solution, Ag nanoparticles, of which the average size was in the range of 2.4 ~ 3 nm, were deposited on the surface of TiO₂ very finely as shown in Fig. 3(a). The existence of Ag was confirmed by the EDS analysis (Table 2). In addition, the lattice fringes of TiO₂ and Ag are observed in the high-resolution TEM images as illustrated in Fig. 4 and the values of lattice spacing were examined with SAED patterns as shown in inset images of Fig. 4. The prepared TiO film was comprised of crystalline TiO₂ with the lattice spacing value of 0.346 nm, which

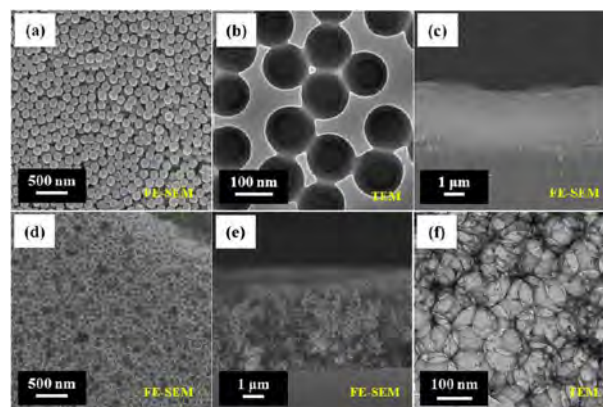


Fig. 2. FE-SEM and TEM images of (a, b) PS particles synthesized by emulsifier-free emulsion polymerization method, (c) PS template film fabricated by dip coating, and (d-f) TiO film fabricated after PS template was eliminated by heat treatment (d: top view, e: side view).

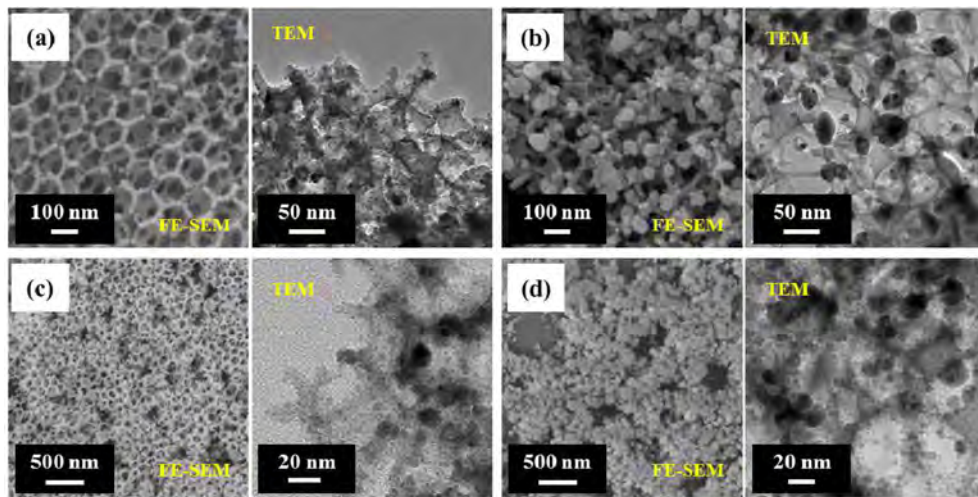


Fig. 3. FE-SEM and TEM images of (a) AT10, (b) ATA10, (c) AT30, and (d) ATA 30 films.

Table 2. EDS data of prepared samples (atomic %).

Element	AT10	ATA10	AT30	ATA30
O K	55.99	58.40	49.07	56.42
Si K	27.41	27.18	31.02	27.41
Ti K	3.71	1.45	4.05	1.65
Ag L	0.77	0.89	1.96	2.56

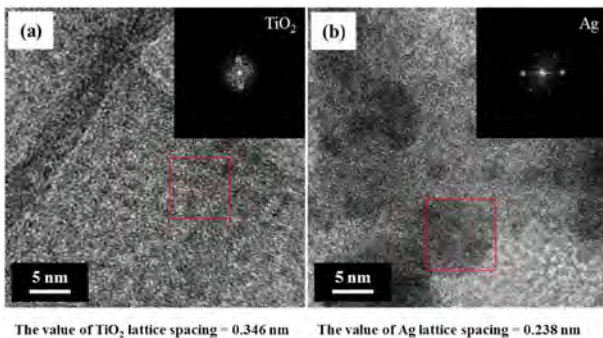


Fig. 4. HR-TEM images of (a) TiO₂ film and (b) AT30 film. Insets are SAED patterns of each sample.

corresponds to the (101) plane of anatase phase of TiO₂ (JCPDS 21-1272). Furthermore, the observed lattice spacing of 0.238 nm at AT film corresponds to the (111) plane of cubic phase of Ag (JCPDS 04-0783). From these experimental results, it was confirmed that Ag nanoparticles were introduced on the surface of TiO₂ films successfully through photodeposition method under UV irradiation.

Effect of APTMS treatment

APTMS is generally used as a chemical binder to attach metal nanoparticles on the surface of oxides [22, 23]. Thus, the effect of APTMS treatment on the Ag coating process was also studied.

The fine Ag nanoparticles, which was about

2.4 ~ 3 nm, were deposited on the TiO₂ film without APTMS treatment (Fig. 3(a) and (c)). On the other hands, Fig. 3(b) and (d) presents the ATA films (Ag-coated TiO₂ films which was treated by APTMS). When the APTMS treatment was performed, large particles were observed and the stable inverse opal structure was not observed in FE-SEM images. However, as a result of TEM analysis, there were 15 ~ 37 nm-sized Ag nanoparticles on the surface of TiO₂ film and the inverse opal structure was maintained after Ag deposition process was performed with APTMS-treated TiO₂ film. In other words, Ag nanoparticles were coated on the surface of TiO₂ film without collapse of the structure. This means that APTMS treatment brought about the deposition of relatively large Ag nanoparticles on the surface of TiO₂ film. This is because the amine groups of APTMS act as attaching/nucleation site for Ag nanoparticles. As a result, Ag nanoparticles are attached to the amine group and large particles are formed by growth of nuclei [23]. EDS data also represents similar result and the values were shown in Table 2. Compared to the ratio of Ag atoms of the TiO₂ films without APTMS treatment (AT10, AT30), the APTMS-treated samples showed the higher atomic ratio of Ag (ATA10, ATA30).

Effect of UV irradiation time

When Ag nanoparticles are coated by using photodeposition method, the UV irradiation time is an important factor. Therefore, the effect of UV irradiation time on the Ag deposition was also investigated and the results are shown in Fig. 3 and Table 2. As shown in Fig. 3, the average size of Ag nanoparticles was not changed significantly with the variation of UV irradiation time. On the other hand, the deposited amount of Ag nanoparticles was increased as UV-light irradiated longer from 10 min to 30 min. Moreover, when the APTMS-treated TiO₂ films were used, the same phenomenon occurred as shown in Fig. 3(c) and

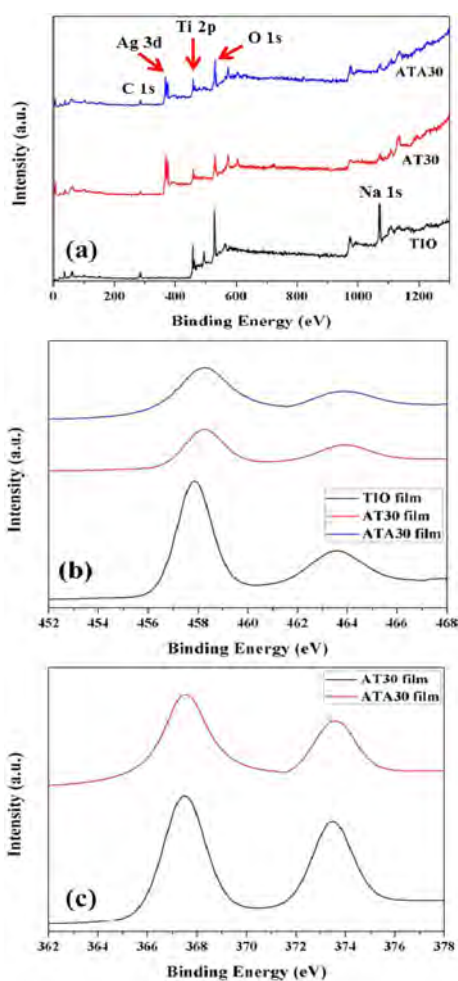


Fig. 5. XPS data of TIO, AT30, and ATA30 films; (a) full-range survey spectra, (b) Ti 2p spectra, and (c) Ag 3d spectra.

(d) as well as Table 2. These results indicate that the photodeposition time affects the amount of Ag deposits strongly.

Analysis of chemical state

To further verify the chemical state of the TIO and Ag-deposited TIO films with or without APTMS treatment (AT or ATA film, respectively), XPS analysis was conducted (Fig. 5). The survey XPS spectra (Fig. 5(a)) show that TIO film contains Ti and O, meanwhile, AT and ATA films are mainly composed of Ti, O and Ag. No other impurities are observed except C and Na. The presence of C is ascribed due to the ex-situ preparation process or adventitious hydrocarbons from the XPS instrument itself [24]. A trace amount of Na peak could appear due to the diffusion of Na atoms existed in the glass substrate into the surface of the films after annealing process.

Fig. 5(b) presents the high-resolution XPS spectra of Ti 2p electron for the TIO, AT30, and ATA30 films. The Ti 2p spectra of TIO consist of two photoelectron peaks assigned to Ti 2p_{3/2} at 457.88 and Ti 2p_{1/2} at 463.98 eV, respectively. The Ti 2p_{3/2} peak of TIO films

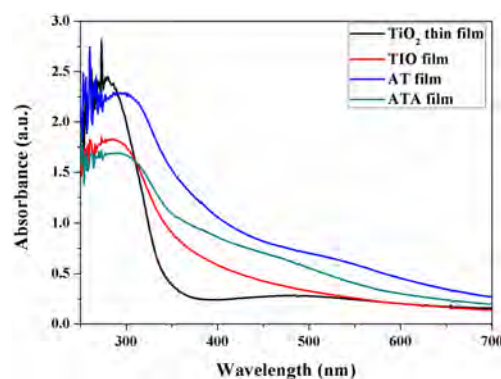


Fig. 6. UV-vis absorption spectra of TIO, AT, and ATA films.

has a lower binding energy compared to that of the anatase phase of pure TiO₂ (459.2 eV), indicating the increase of the electron densities of the Ti atom [25]. On the contrary, after the Ag deposition, the peaks of Ti 2p_{3/2} were shifted to higher binding energy. Because the Fermi level of Ag is lower than the conduction band of TiO₂, the electron transfer should be facilitated from the TiO₂ to the Ag particles and then the outer electron cloud density of Ti ions is decreased [26-28].

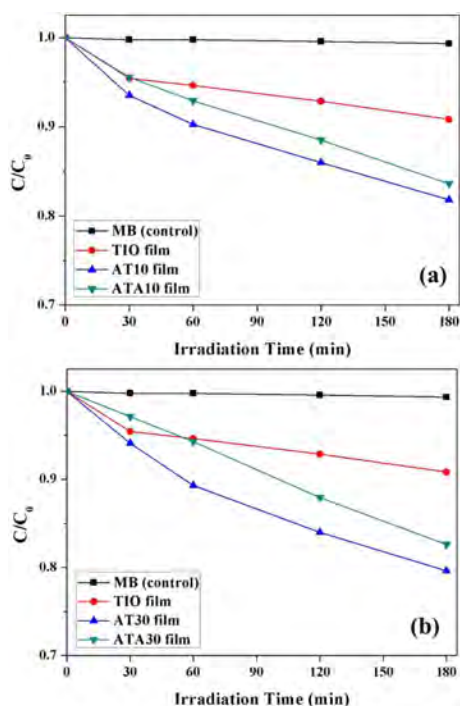
The Ag 3d peaks also appear as a symmetrical doublet in Fig. 5(c). The Ag 3d binding energies of AT and ATA films are 367.68, 367.88 eV (Ag 3d_{5/2}) and 373.58, 373.68 eV (Ag 3d_{3/2}), respectively. The peak separation between the Ag 3d_{5/2} and Ag 3d_{3/2} signals is 6.0 eV, which can be attributed to the cubic phase in Ag particles [29, 30]. These spectra appear to be negatively shifted compared to those of bulk Ag (BE value of 3d_{5/2} and 3d_{3/2} is 368.3 and 374.3 eV, respectively [31]). It suggests that some electrons may be transferred from TiO₂ to Ag, confirming the strong interaction between TiO₂ and Ag nanoparticles in the Ag-deposited TIO films. The interaction between Ag and TiO₂ is expected to result in the effective photogenerated charge separation and should promote photocatalysis [26, 32, 33].

Analysis of optical property

The optical property of TiO₂ is significant because the use of wide light range can lead to high efficiency of photocatalysts. The absorbance of prepared films was measured by using UV-Vis spectrometer and the results were shown in Fig. 6. In the region from 320 to 500 nm, the absorbance of TIO film was higher than that of TiO₂ thin film. It indicates that physical modification of TiO₂ results in the increasing light absorption due to multiple scattering effect of pore structure [34]. After chemical modification with deposition of Ag nanoparticles, the peaks of AT and ATA films have a stronger absorption in the visible light range comparing with the pure TIO film. It demonstrates that these Ag-deposited TIO composite films show an obviously enhanced absorption property in the visible light range due to surface plasmon absorption (SPA) effect corresponding to Ag nanoparticles on the surface of TiO₂ [35, 36]. In

Table 3. Photocatalytic efficiencies of each sample after 180 min.

Samples	Reference	TiO	AT10	ATA10	AT30	ATA30
Photocatalytic efficiency (%)	0.69	9.18	18.19	16.38	20.37	17.40

**Fig. 7.** Photocatalytic performance of different samples with Ag deposition time (a) for 10 min, and (b) for 30 min.

addition, the absorption spectra of Ag-deposited TiO₂ films have a red shift, which should be attributed to the presence of the contact between Ag nanoparticle and TiO₂ and the increasing charge-transfer between them [37]. However, the absorbance of ATA film is much lower than that of AT film because the large Ag particles lower the SPA effect [38-40]. Moreover, the large Ag particles shield the surface of TiO₂ and the light absorption of TiO₂ is interrupted [41].

Measurement of the photocatalytic activity

The photodegradation of MB in aqueous solution was used to estimate the photocatalytic activities of fabricated films and their photocatalytic efficiencies after 3 h were summarized in Table 3. The relative concentration C/C_0 of MB solution was plotted against UV irradiation time for various TiO₂ films (Fig. 7). It is observed that there was no MB degradation in the absence of a photocatalyst. Overall, the photocatalytic efficiencies of the samples showed lower value. These results may be ascribed to very small amount of TiO₂ consisting of the prepared films. The photocatalytic activities of the prepared TiO₂ films vary in the following order: AT film > ATA film > pure TiO₂ film. It can be seen that the deposition of Ag nanoparticles enhanced photocatalytic activity of TiO₂ obviously

because a Schottky barrier was formed at the interfaces between TiO₂ and Ag nanoparticles, leading to better separation of charge carriers [41]. However, when the large Ag nanoparticles were deposited to the films due to the APTMS treatment (ATA10, ATA30), relatively low photocatalytic efficiency was obtained compared to the films without APTMS treatment (AT10, AT30). This is because the large Ag nanoparticles inhibit the SPA effect and influence the decrease in not only the optical absorption but photocatalytic activity [42]. On the other hand, the photocatalytic efficiency was also influenced by the amounts of Ag nanoparticles immobilized on the TiO₂ film and it can be confirmed by comparing that of the samples prepared with different UV irradiation time. When the UV irradiation time of photodeposition process increased, the amount of Ag nanoparticles increased and the photocatalytic efficiencies also increased from 18.19% (AT10) to 20.37% (AT30). This result was also observed in that of APTMS-treated TiO₂ films. The photocatalytic efficiency of ATA10 was 16.38% while that of ATA30 was 17.40%. It demonstrates that a large amount of Ag nanoparticles could reduce the rate of carrier recombination of TiO₂ and improve the photocatalytic activity.

Conclusions

In summary, the TiO₂ inverse opal films coated with silver nanoparticles were successfully fabricated on the glass substrates. As shown in FE-SEM images, the multi-layered PS template was prepared from self-assembled spherical and monodisperse PS nanoparticles. The 3D-ordered inverse opal structure with a pore diameter of approximately 114 nm was observed in FE-SEM and TEM images. After deposition of Ag onto the surface of TiO₂ film, the existence of Ag can be confirmed by HR-TEM, XPS, and EDS analyses. As the surface of TiO₂ was modified by APTMS treatment before Ag deposition process, the large Ag particles were introduced on the TiO₂ film due to stronger interaction between metal and amine group of APTMS. The test results for the photocatalytic performances of fabricated films showed that Ag-deposited TiO₂ film exhibited enhanced photocatalytic efficiency relative to pure TiO₂ film. The enhanced photocatalytic activity was attributed to Ag nanoparticles playing a role in not only improving the light absorption property but decreasing in carrier recombination. However, the Ag-deposited TiO₂ film with APTMS treatment obtained lower photocatalytic efficiency than pure Ag-deposited TiO₂ film because APTMS treatment induced the formation of large Ag particles and the excessive coverage of the TiO₂ by Ag deposits decreased the absorption property.

Acknowledgment

This work was supported by the New & Renewable

Energy Program of the Korea Institute of Energy Technology Evaluation and Planning (KETEP) grant funded by the Korea government Ministry of Trade, Industry & Energy (No. 20113010010030).

References

1. B. Oregan and M. Gratzel, *Nature* 353 (1991) 737-740.
2. O.K. Varghese, D. Gong, M. Paulose, K.G. Ong, E.C. Dickey and C.A. Grimes, *Adv. Mat.* 15 (2003) 624-627.
3. M. Wagemaker, R. van de Krol, A.P.M. Kentgens, A.A. van Well and F.M. Mulder, *J. Am. Chem. Soc.* 123 (2001) 11454-11461.
4. A. Fujishima, T.N. Rao and D.A. Tryk, *J. Photochem. Photobiol. C* 1 (2000) 1-21.
5. E. Pelizzetti, C. Minero, V. Maurino, A. Sclafani, H. Hidaka and N. Serpone, *Environ. Sci. Technol.* 23 (1989) 1380-1385.
6. U. Diebold, *Surf. Sci. Rep.* 48 (2003) 53-229.
7. S. Sato, *Chem. Phys. Lett.* 123 (1986) 126-128.
8. U.I. Gaya and A.H. Abdullah, *J. Photochem. Photobiol. C* 9 (2008) 1-12.
9. B.T. Holland, C.F. Blanford and A. Stein, *Science*, 281 (1998) 538-540.
10. Q.B. Meng, C.H. Fu, Y. Einaga, Z.Z. Gu, A. Fujishima and O. Sato, *Chem. Mater.* 14 (2002) 83-88.
11. J. Liu, T. An, G. Li, N. Bao, G. Sheng and J. Fu, *Micropor. Mesopor. Mater.* 124 (2009) 197-203.
12. A.L. Linsebigler, G. Lu and J.T. Yates, *Chem. Rev.* 95 (1995) 735-758.
13. X.Z. Li and F.B. Li, *Environ. Sci. Technol.* 35 (2001) 2381-2387.
14. P.D. Cozzoli, E. Fanizza, R. Comparelli, M.L. Curri and A. Agostiano, *J. Phys. Chem. B* 108 (2004) 9623-9630.
15. W. Lu, S. Gao, and J. Wang, *J. Phys. Chem. C* 112 (2008) 16792-16800.
16. C. Ren, B. Yang, M. Wu, J. Xu, Z. Fu, Y. Lv, T. Guo, Y. Zhao and C. Zhu, *J. Hazard. Mater.* 182 (2010) 123-129.
17. S.M. Morton, D.W. Silverstein and L. Jensen, *Chem. Rev.* 111 (2011) 3962-3994.
18. Y. Fu, Z. Jin, Y. Ni, H. Du and T. Wang, *Thin Solid Films*, 517 (2009) 5634-5640.
19. D.W. Kim, J.M. Lee, C. Oh, D.S. Kim, S.G. Oh, *J. ColloidInterfaceSci.* 297 (2006) 365-369.
20. C.F. Lao, Z.Z. Chu and D.C. Zou, *Acta Phys. Chim. Sin.* 27 (2011) 419-424.
21. D. Knopp, D. Tang and R. Niessner, *Anal. Chim. Acta* 647 (2009) 14-30.
22. J.Z. Xu, W.B. Zhao, J.J. Zhu, G.X. Li and H.Y. Chen, *J. Colloid Interface Sci.* 290 (2005) 450-454.
23. T.H. Kim, D.W. Kim, J.M. Lee, Y.G. Lee and S.G. Oh, *Mater. Res. Bull.* 43 (2008) 1126-1134.
24. G. Liu, W. Jaegermann, J. He, V. Sundstrom and L. Sun, *J. Phys. Chem. B* 106 (2002) 5814-5819.
25. J. Xu, B. Yang, M. Wu, Z. Fu, Y. Lv and Y. Zhao, *J. Phys. Chem. C* 114 (2010) 15251-15259.
26. B. Xin, L. Jing, Z. Ren, B. Wang and H. Fu, *J. Phys. Chem. B* 109 (2005) 2805-2809.
27. J. Li, J. Xu, W. Dai and K. Fan, *J. Phys. Chem. C* 113 (2009) 8343-8349.
28. L. Mai, D. Wang, S. Zhang, Y. Xie, C. Huang and Z. Zhang, *Appl. Surf. Sci.* 257 (2010) 974-978.
29. C. Sella, S. Chenot, V. Reillon and S. Berthier, *Thin Solid Films* 517 (2009) 5848-5854.
30. B. Lv, Y. Xu, H. Tian, D. Wu and Y. Sun, *J. Solid State Chem.* 183 (2010) 2968-2973.
31. J.F. Moulder, W.F. Stickle, P.E. Sobol, and K.D. Bomben, *Handbook of X-ray Photoelectron Spectroscopy*, Perkin-Elmer Co., Eden Prairie, MN, USA (1992).
32. J. Yu, J. Xiong, B. Cheng and S. Liu, *Appl. Catal. B* 60 (2005) 211-221.
33. L. Yang, X. Jiang, W. Ruan, J. Yang, B. Zhao, W. Xu and J.R. Lombardi, *J. Phys. Chem. C* 113 (2009) 16226-16231.
34. S. Hore, P. Nitz, C. Vetter, C. Prah, M. Niggemann and R. Kern, *Chem. Commun.* 15 (2005) 2011-2013.
35. J.M. Herrmann, H. Tahiri, Y. Ait-Ichou, G. Lassaletta, A.R. González-Elipe and A. Fernandez, *Appl. Catal. B* 13 (1997) 219-228.
36. W. Wang and S.A. Asher, *J. Am. Chem. Soc.* 123 (2001) 12528-12535.
37. R.T. Tom, A.S. Nair, N. Singh, M. Aslam, C.L. Nagendra, R. Philip, K. Vijayamohan and T. Pradeep, *Langmuir* 19 (2003) 3439-3445.
38. C.L. Haynes and R.P. van Duyne, *J. Phys. Chem. B* 105 (2001) 5599-5611.
39. J.J. Mock, M. Barbic, D.R. Smith, D.A. Schultz and S. Schultz, *J. Chem. Phys.* 116 (2002) 6755-6759.
40. Y. Ohko, T. Tatsuma, T. Fujii, K. Naoi, C. Niwa, Y. Kubota and A. Fujishima, *Nat. Mater.* 2 (2003) 29-31.
41. Z. Shan, J. Wu, F. Xu, F.Q. Huang and H. Ding, *J. Phys. Chem. C* 112 (2008) 15423-15428.
42. V. Vamathevan, R. Amal, D. Beydoun, G. Low and S. McEvoy, *J. Photochem. Photobiol. A* 148 (2002) 233-245.